Experimental hydraulics on fish-friendly trash-racks: an ecological approach

Marcell Szabo-Meszaros [a,*], Christy Ushanth Navaratnam [a], Jochen Aberle [a,b], Ana T. Silva [c], Torbjørn Forseth [c], Olle Calles [d], Hans-Petter Fjeldstad [e], Knut Alfredsen [a]

[a] Department of Civil and Environmental Engineering, NTNU, S. P. Andersens 5, Trondheim 7491, Norway

[b] Leichtweiß-Institut für Wasserbau, Technische Universität Braunschweig, 38106 Braunschweig, Germany

[c] Norwegian Institute for Nature Research (NINA), Høgskoleringen 9, Trondheim 7043, Norway

[d] Department of Biology, Karlstad University, S-651 88 Karlstad, Sweden

[e] SINTEF Energy Research, Sem Sælandsvei 11, Trondheim 7048, Norway

[*] Corresponding author at: Department of Civil and Environmental Engineering, NTNU, S. P. Andersens 5, Trondheim 7491, Norway. Tel.: +47 735 92 415; mobile: +47 932 85 521. E-mail address: marcell.szabo-meszaros@ntnu.no (M. Szabo-Meszaros).

Abstract

The obstruction of fish migratory routes by hydroelectric facilities is worldwide one of the major threats to freshwater fishes. During downstream migration, fish may be injured or killed on the trash-racks or in the hydropower turbines. Fish-friendly trash-racks that combine both ecological and technical requirements are a solution to mitigate fish mortality at a low operational cost. This study presents results from an experimental investigation of head-losses and the hydrodynamic performance of six angled trash-rack types with 15 mm bar spacing, varying bar-setup (vertical-streamwise, vertical-angled and horizontal bars) and bar profiles (rectangular and drop shape) under steady flow conditions. The trash-racks were positioned at 30° to the wall of the flume and combined with a bypass at their downstream end. The impact of the different trash-rack types on the upstream flow field was characterized using Image based Volumetric 3-component Velocimetry (V3V) and at the bypass-entrance using an Acoustic Doppler Velocimeter (ADV). The results show that trash-racks with vertical-streamwise and horizontal oriented bars with drop-shape profiles have similar head-losses (13% difference), while trash-racks with vertical-angled bars provide 3-8 times larger head-losses compared to the remaining configurations. The velocity measurements showed that the highest flow velocities occurred for configurations with vertical-angled bars (0.67 m s^{-1} and 0.81 m s^{-1} on average, respectively). Turbulence related parameters (e.g. Reynolds shear stresses and Turbulent kinetic energy) were also investigated to evaluate the performance of the alternative trash-racks from both, engineering and ecological perspectives.

Keywords: flow hydrodynamics, intake, turbulence, V3V, fish migration

1. Introduction

River fragmentation by hydroelectric facilities is a well-known phenomenon affecting native migratory fish (Larinier, 2001). For example, the populations of anadromous Atlantic salmon (*Salmo salar*) and the endangered catadromous European eel (*Anguilla Anguilla*) decreased significantly in Europe due to the hydropower dams (Hindar et. al., 2003, ICES, 2001). This problem is typically associated with the demanding passage through the artificial barriers in both up- and downstream directions (Calles and Greenberg, 2009, Larinier, 2008, Lundqvist et al., 2008, Martignac et al., 2013). During downstream migration, fish face diverted paths as the streamflow is divided at the intake of a hydropower plant (HPP). The entrance to the intake channel is in most cases equipped with trash-racks to protect the turbines from debris, sediment and floating ice (Mosonyi, 1991). They are typically perpendicularly oriented to the flow with 50-150 mm bar spacing (Mosonyi, 1991) and can therefore, besides their operational purpose, be used to prevent larger fish from entering the intake of a HPP. The trash-racks can affect migrating fish as they delay migration significantly or cause injuries, sometimes lethal, depending on the size and type of the HPP and its intake structures (Bruijs and Durif, 2009). The mortality associated with hydropower intakes and turbines may be high when fish are either small enough to swim/drift through the trash-rack bars and pass through the turbines or large enough to be pinged onto the trash-rack surface in cases when the approach flow exceeds their swimming capability (Adam and Bruijs, 2006). One solution is the adoption of alternative designs of trash-racks, which prevents both rack passage, impingement and guide the fish towards a bypass (Calles et al., 2013).

Several studies have explored different fish friendly trash-racks designs (Amaral et al., 2002, Boubee and Williams, 2006, Larinier, 2008). One approach is to reduce the bar spacing to prevent juvenile fish from passing through the bars (Bruijs and Durif, 2009), another is to incline the trash-racks from the bottom (so called inclined trash-racks) or angle them to the side (so called angled trash-racks) (DWA, 2005). These designs can be also used to guide the fish either to the surface (at inclined trash-racks), or to the side of the trash-rack (at angled trash-rack types) where the fish may circumvent the obstacle using a bypass channel (Calles et al., 2012). Other studies tested the barsin different positions (Albayrak et al., 2017, Tsikata et al., 2014). The study of Boes et al. (2016) indicated that trash-racks with horizontal bars combined with a bypass can be a preferable solution for fish protection at smaller HPPs, while trash-racks with vertical bars can be an alternative for larger HPPs. The design of an optimal solution taking into account economy and ecology requires the consideration of a number of abiotic parameters such as head-losses and maintenance. In this context, Raynal et al. (2013) investigated the effect of bar-alignment (vertically streamwise oriented bars and vertically angled bars so called 'classical' trash-racks) on head losses and flow characteristics upstream of the trash-racks. They found that trash-racks with vertically angled bars are characterized by significantly larger head-losses and higher velocities at the upstream side of the trash-racks.

The efficiency of a bypass for downstream passage of fish is strongly dictated by the hydraulic conditions at the entrance of the structure, which vary with the design of the associated trash-racks. The effect of hydrodynamics of the flow on the swimming performance and behavior of fish has long been recognized (Kroese et al., 1978, Kroese and Schellart, 1992). Fish can detect water motions in their immediate surroundings by using neuromasts, that can be located superficially all over the fish skin (superficial neuromasts) or under the skin in the head and along the length the fish (canal neuromasts). Superficial neuromasts have been shown to respond to changes in external flow velocity while canal neuromasts respond to variations in external flow acceleration (related with changes in external flow pressure) (Chagnaud et al., 2007, Kroese et al., 1978, Kroese and Schellart, 1992, Barbier and Humphrey, 2009). Thus, it is imperative to improve knowledge on the hydraulic conditions at the vicinity of trash-racks and associated bypasses.

Besides the standard flow characteristics (e.g. time-averaged velocity distributions) typically explored in trash-rack experiments ((Albayrak et al., 2017, Tsikata et al., 2009), turbulent flow characteristics may be important for fish movement and the tolerance and preferences of fish to the surrounding flow patterns (Drucker and Lauder, 1999, Silva et al., 2016). Fish are also known to react to flow heterogeneity on smaller distances of centimeters to body length (Enders et al., 2012), which can compromise their orientation, stability and swimming capacity, concomitantly increasing the energetic costs associated to swimming (Silva et al., 2016). For instance, Tritico (2009) found that vortexes play a critical role for fish swimming stability showing that more detailed analysis of flow patterns offer better understanding of the flow conditions from fish perspectives. Moreover, several studies have shown that turbulence parameters such as turbulent kinetic energy and Reynolds stress can be essential to seize the difference between fish preferences and repulsion (Enders et al., 2003, Liao, 2007, Silva et al., 2011). Turbulent flow characteristics can be determined in experiments with trash-racks by using advanced measurement technologies such as Particle Image Velocimetry (PIV) (e.g. Raynal et al., 2013, Sayeed-Bin-Asad, 2009, Tsikata et al., 2009).

Here we explored the head-losses and the hydrodynamic performance of six angled trash-rack designs with varying bar-angles, -profiles and -orientation under steady flow conditions using a combination of Acoustic Doppler Velocimeter (ADV) and Volumetric 3-component Velocimetry techniques. This facilitated a detailed study of the hydrodynamics of the flow for different trash-racks configurations and associated bypasses. The hydraulic results are discussed in relation to existing knowledge on behavioral responses of salmonid smolts and silver eels, and the operational feasibility of the designs.

2. Materials and methods

2.1. Experimental setup

Experiments were carried out in a 1.0 m-wide, 12.5 m-long and 1.0 m-deep recirculating flume in the hydraulic laboratory of the Norwegian University of Science and Technology. In the experiments, the horizontal flume bed was smooth (plastic-bed) and the glass-sided walls provided visual access to the flow. Discharge was measured with inductive discharge meters in the return-pipes to the flume-inlet and water depths in the flume were measured at four locations along the flume using piezometers (P_1 to P_4) installed at the flume centerline and at distances of x = 8.125, 6.875, 5.625, and 3.125 m, respectively from the flume inlet.

The tested trash-racks were 1.7 m long and 0.9 m wide and were installed in the middle section of the flume (x = 7.06 m from the inlet) with an inclination of *ß* = 30° to the wall (Fig. 1), a setup which had also been tested by Raynal et al. (2013) and Albayrak et al. (2017). Two different bar shapes (rectangular (PR) and hydrodynamic (PH) – based on Raynal et al. (2013) (Fig. 1b) were tested for three different bar-setups: (i) vertical bars aligned with the flow (streamwise orientation- racks I and II), (ii) vertical bars, angled 60º to the flow (hence perpendicular to the trash-rack main axis; racks III and IV), and (iii) horizontal orientated bars (racks V and VI) (Table 1). The bar width (b), length (L) and the space between bars (e) were of 8 mm, 64 mm and 15 mm, respectively. The ratio of bar to flume width used in this study was chosen in accordance with the criteria used by Raynal et al. (2013). Moreover, the bar spacing of 15 mm was adapted from Nyqvist et al. (2017) who indicated that such a bar spacing improves downstream passage of salmonid kelts.

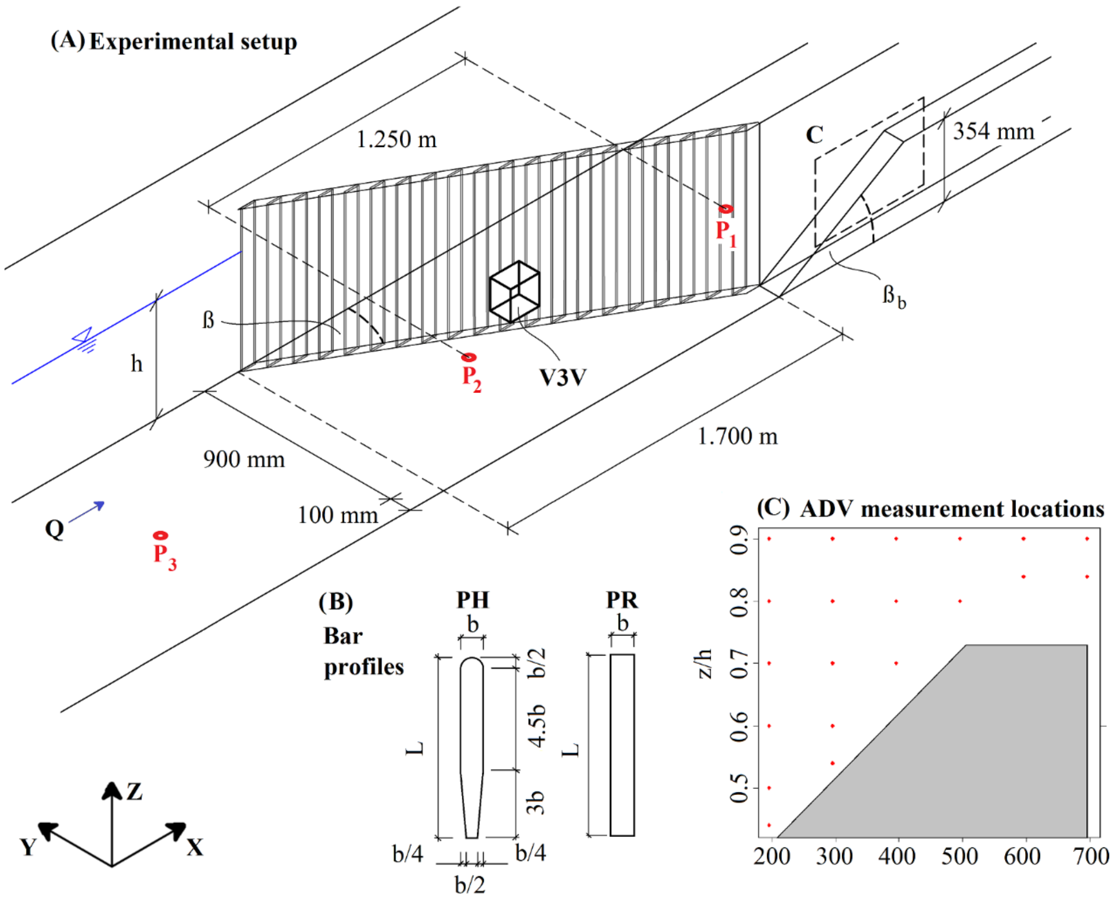

Fig. 1. Experimental setup and sampling locations in a straight open-channel. (A) The position of the trash-rack and the surrounding elements: bypass at the downstream end of the grid, the P_1-P_3 piezometers and the sampled volume of the V3V measurements. (B) The locations of the velocity measurements at the entrance of the bypass section, using ADV. The coordinate system of the bypass is originated at the bottom of the ramp. (C) The adapted bar profiles for the experiments: rectangular (PR) on the right and hydrodynamic shape (PH) on the left.

A bypass-structure was constructed at the downstream end of the trash-racks (Fig. 1a). The bypass consisted of an entrance ramp with an angle of $ß_b$ = 30° and a bypass channel of 100 mm width elevated 354 mm from the bottom of the flume. The ramp design was based on results of Silva et al. (2016) in a study on the downstream swimming behavior of the European eel (*Anguilla anguilla*) and Iberian barbel (*Barbus bocagei*) over modified spillways. The flow in the bypass was separated from the main flow in the flume by a 4 m long and 8 mm thick wall. The bypass-structure was a fixed element in all the experiments and the flow rate through the bypass was determined from flow velocity measurements (see further below).

All experiments were carried out with a water depth of h = 500 ± 5 mm. The water levels during the experiments were determined using the aforementioned piezometers. Friction losses associated with the flume structure (Δh_0) were determined in preliminary tests without trash-racks for four flow discharges (Q = 0.11, 0.14, 0.17, and 0.20 $m^3\ s^{-1}$). Head-losses Δh associated with the different trash-rack setups were determined according to $\Delta h = \Delta H - \Delta h_0$, where ΔH is the water level difference between piezometers P_3 and P_1 located up- and downstream of the trash-rack, respectively (see Fig. 1). The corresponding head-loss coefficient (ξ) was computed according to $\Delta h = \xi v_{b3}^2/2g$, where v_{b3} is the calculated bulk velocity (cross-sectional averaged velocity) at P_3 and g is the gravitational acceleration (9.81 m s^{-2}). The volume-based blockage ratio (O_{bV}) was calculated according to:

$$O_{bV} = \frac{O_{sV}}{O_{wV}} \quad (1)$$

where O_{sV} is the total volume of solid materials inside the control section and O_{wV} is the total volume of the control section. The control section was defined based on a 500 mm high and 64 mm wide parallelogram polygon, i.e. according to the enclosing volume of rack III. We considered this as an adequate standardized method to characterize flow blockage for the different trash-racks taking into account the overall trash-rack structure and not only the projected structure (Table 1).

2.2. Flow velocity and turbulence measurements

Velocity measurements at the entrance of the bypass channel were conducted using a down-looking Nortek Vectrino+ 3D Acoustic Doppler Velocimeter (ADV). The ADV was installed on an automated traverse system aligned with the centerline of the bypass channel. Overall, 20 sampling points, equally distributed in the streamwise and vertical direction across the ramp were measured (Fig. 1c) for a duration of 60 seconds and with a sampling frequency of 50Hz. The acquired ADV-data were post-processed using WinADV (Wahl 2002) applying phase-space threshold despiking according to Goring and Nikora (2002). The minimum correlation was set to 70% while the minimum signal-to-noise ratio (SNR) level was set to 15 dB following Lane et al. (1998) and McLelland and Nicholas (2000). Sampling locations at which at least 30% of the velocity time-series was filtered out during despiking were discarded from further analyses. The ADV-data were used to calculate resultant velocities ($v_r = \sqrt{v_x^2 + v_y^2 + v_z^2}$ where v_x, v_y and v_z are the velocity components in *x*, *y* and *z* directions, respectively). The measurement grid size was 100 mm along the *x*, and 30-50 mm along the *y* axis.

Velocity measurements upstream of the trash-racks were carried out using the volumetric 3-component particle image-velocimetry system (V3V) of TSI. These measurements were carried out at the center of the trash-racks (in both transverse and vertical direction) to minimize disturbances from the flume walls and the free surface. The V3V-system consisted of a pulsed laser (Nd:YAG type, power output: 400 mJ) and three-aperture, 4-Mega-pixel CCD cameras which were mounted outside of the flume. The V3V-system provided instantaneous velocity measurements in a 140x100x140 mm target volume in the *x*, *y* and *z* directions, respectively (voxel size: 2 mm), which were taken for a period of 200 seconds with a sampling frequency of 15 Hz. For the measurements, the flow was seeded with small polyamide particles with a diameter of 55 µm. The *Insight V3V 4G* software was used to post-process the V3V data (see detailed information about the method in Pothos et al. 2009). The size of each V3V dataset was reduced by removing the first three layers of cells at each face of the sampling cube due to the low reliability of these values at the boundaries. Based on data quality and experimental conditions, the size of the datasets varied between 100,000 and 130,000 measured instantaneous velocities within the sampled volume. In order to reduce the effect of outliers on the analysis only velocities were considered within the 0.1st and 99.9th percentiles of the velocity probability distribution. The V3V data was also used to calculate the normal velocities (v_n, perpendicular to the trash-rack) at the immediate upstream side of the racks as $v_n = v_x * \sin(ß) + v_y * \cos(ß)$.

Velocity measurements (both ADV and V3V) were carried out for flow discharges *Q*= 0.17 and 0.20 m^3 s^{-1}. For the following analysis, bulk flow conditions used for normalization of hydrodynamic parameters were determined at cross-section P_4 assuming that this cross-section remained largely unaffected by the trashrack. For example, the bulk velocity at this cross-section was used to calculate bar Reynolds number $R_b = b * v_{b4}/\nu$, where ν is the kinematic viscosity of the water (10^{-6} m^2 s^{-1}) (Table 1).

The high resolution ADV- and V3V data were used to calculate the turbulent kinetic energy (*TKE*) according to $TKE = \frac{1}{2} * (\overline{u'^2} + \overline{v'^2} + \overline{w'^2})$ where *u'*, *v'* and *w'* are the velocity fluctuations components in the streamwise (*x*), transverse (*y*) and vertical (*z*) directions, respectively, and the overbar denotes temporal averaging (Nezu and Nakagawa, 1993). Reynolds shear stresses were defined for the streamwise, horizontal ($\tau_{u'v'}$) and vertical planes ($\tau_{u'w'}$) according to $\tau_{u'v'} = -\rho\overline{u'v'}$ and $\tau_{u'w'} = -\rho\overline{u'w'}$, where ρ denotes the water density (1000 kg m^{-3}). The acceleration components in the x, y and z direction (a_u, a_v, a_w, respectively) were computed according to:

$$a_u = \bar{U} * \frac{\delta\bar{U}}{\delta x} + \bar{V} * \frac{\delta\bar{U}}{\delta y} + \bar{W} * \frac{\delta\bar{U}}{\delta z}$$

$$a_v = \bar{U} * \frac{\delta\bar{V}}{\delta x} + \bar{V} * \frac{\delta\bar{V}}{\delta y} + \bar{W} * \frac{\delta\bar{V}}{\delta z} \quad (2)$$

$$a_w = \bar{U} * \frac{\delta\bar{W}}{\delta x} + \bar{V} * \frac{\delta\bar{W}}{\delta y} + \bar{W} * \frac{\delta\bar{W}}{\delta z}$$

where $\bar{U}, \bar{V}, \bar{W}$ are the time-averaged velocity components in the x, y and z direction, respectively. The resultant acceleration (a_r) was calculated as $a_r = \sqrt{a_u^2 + a_v^2 + a_w^2}$.

In addition to turbulent kinetic energy and the convective acceleration, both the skewness and kurtosis were calculated using R scripts (R Development Core Team, 2017), while the curl (*Ω*) was calculated using Matlab R2016a (MATLAB, 2016) according to:

$$\Omega_x = \frac{\delta W}{\delta y} - \frac{\delta V}{\delta z} \;\; ; \;\; \Omega_y = -\frac{\delta W}{\delta x} + \frac{\delta U}{\delta z} \;\; ; \;\; \Omega_z = \frac{\delta V}{\delta x} - \frac{\delta U}{\delta y} \quad (3)$$

where $\Omega_x, \Omega_y, \Omega_z$ are the curl determination to the x, y and z directions respectively. The curl magnitude (Ω) was calculated as $\Omega = \sqrt{\Omega_x^2 + \Omega_y^2 + \Omega_z^2}$. Note that in the present paper we focus on the curl rather than vorticity in order to investigate the curl of the temporally averaged flow field (streamlines) instead of the instantaneous flow field. Local minima and maxima of the curl field were determined based on the following criteria:

$$\left\{\frac{d\Omega}{dx}; \frac{d\Omega}{dy}; \frac{d\Omega}{dz}\right\} = 0 \quad (4)$$

The number of identified local minima and maxima, $I_{mi\text{-}ma}$ is herein used as an indicator of the local changes in rotational direction inside of the sampling volume.

2.3. Method of ecological evaluation

In order to assess the ecological performance of the tested trash-rack configurations the hydrodynamic parameters from the measurements were combined with the literature data on fish responses to hydraulic conditions (e.g Enders et al., 2012, Lacey et al., 2012, Larinier, 2002, Silva et al., 2011, 2012, Williams et al. 2012).

3. Results

In the following, we present results for the highest flow discharge Q = 0.200 m^3 s^{-1} only, as similar patterns were observed for the experiments conducted at 0.170 m^3 s^{-1}. Head-losses and respective head-loss coefficients are analyzed for all the tested flow discharges.

3.1. Head-loss related parameters

Fig. 2 provides an overview of measured head-losses and head-loss coefficients and reveals differences between the tested trash-rack configurations. Trash-racks with vertical-angled bars (racks III and IV) provided 3-7 times larger Δh values compared to the other trash-rack configurations. Differences were also found between rack I and V (43% difference in head-loss) which are trash-racks with a PR bar shape. The effects of bar shape on both head losses and head-loss coefficients were also observed when the former configurations were tested with PH bars. At the same configurations but with PH bars the difference in head-loss dropped from 43% to 13% between rack II and VI. Therefore, the head-loss difference between trash-rack configurations was lower at configurations with PH bars.

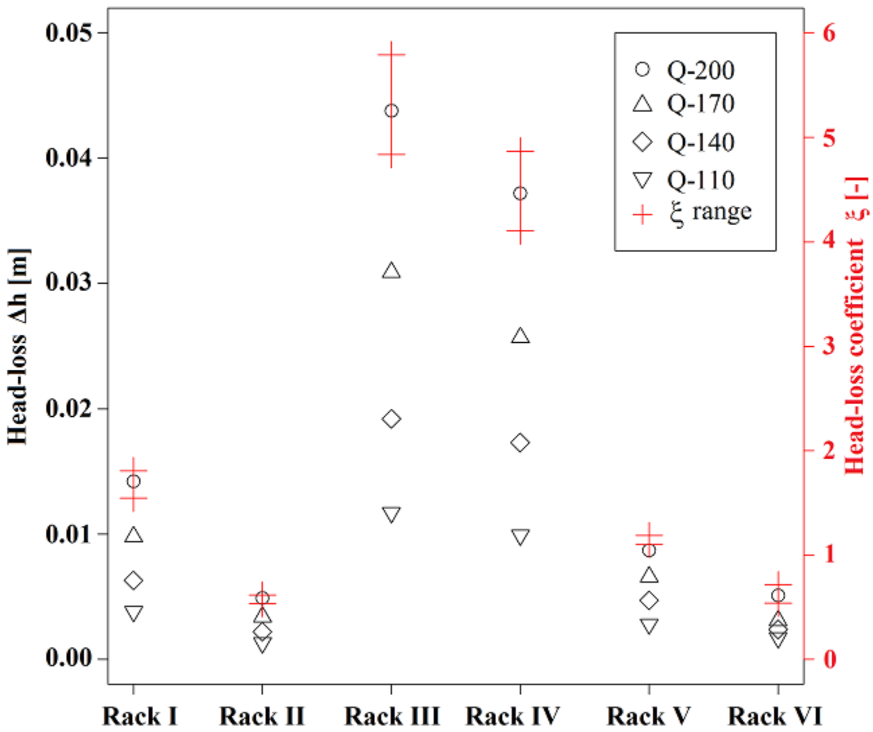

Fig. 2. Head-loss values (m) under different flow rates from 0.110 up to 0.200 m^3 s^{-1} for the tested trash-rack types. The range of the head-loss coefficients (-) according to the different trash-racks are presented in red.

3.2. Bypass section

The flow rate through the bypass was measured based on flow velocity measurements. The Q_b (Table 1) was doubled in configurations tested with vertical-angled bars compared to all the other trash-rack configurations. The discharge reduction was the lowest at both rack II and at rack VI.

Normalized velocity fields ($v_r^* = v_r/v_{b4}$) at the entrance of the bypass section are shown in Fig. 3a, b and c, for rack I, III and V, respectively. Considering that no significant differences in velocity patterns between PR and PH trash-rack types could be identified, Fig. 3 presents the velocity fields for the PR trash-racks. The largest velocities were observed at the ramp crest for all tested configurations. Similar patterns were observed between rack I and rack V, with normalized velocities ranging from 0.4 to 1.5 (v_r range: 0.16 m s^{-1} - 0.60 m s^{-1}) and 0.4 to 1.1 (v_r range: 0.16 m s^{-1} - 0.44 m s^{-1}), respectively. Rack III created the highest velocities (v_r range: 0.31 m s^{-1} - 0.81 m s^{-1}, v_r^* range: 0.8-2.1), which peak (~2.1) which was two times larger than the maximum values found at rack V (1.0-1.2 at the top of the ramp).

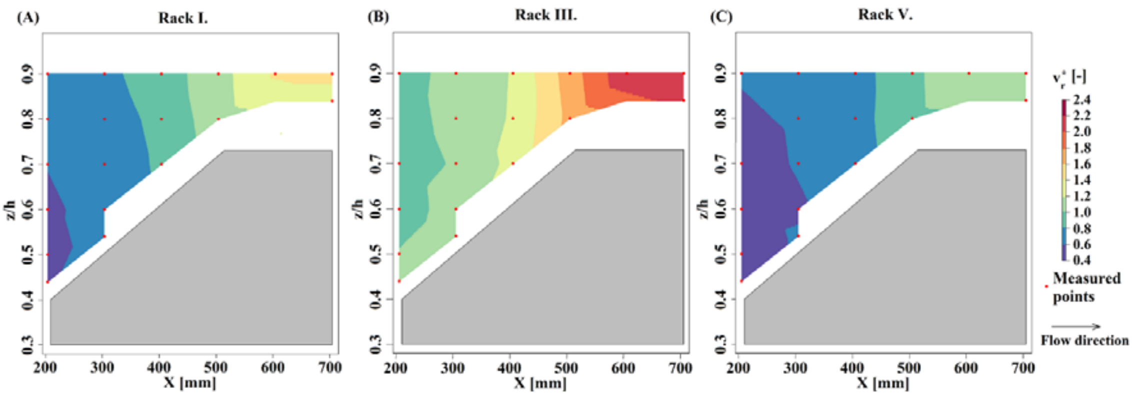

Fig. 3. Interpolated velocity fields at the entrance of the bypass section for (A) rack I, (B) rack III and (C) rack V. The interpolation is based on the normalized resultant velocities (v^*); each locations where the filtered ADV data were valid are presented on the figures (red dots).

Acceleration (see equation 2) was calculated between adjacent measurement points (Table 2). As for the flow velocities, the largest values were observed at the crest of the ramp. Moreover, largest accelerations were observed for trash-racks with vertical-angled bars (rack III and IV), for which acceleration values were 2 to 4 times higher than for the other configurations. The lowest a_r was observed for the experiments with rack VI.

Due to the constriction of the bypass-flow by the ramp and the narrow channel geometry, vertical Reynolds shear stress ($\tau^*_{u'w'} = \tau_{u'w'}/\rho v_{b4}^2$) was analyzed at the entrance of the bypass (Table 2). Trash-racks with horizontal bars provided larger range of vertical Reynolds shear stress compared to the other configurations. Rack I and II had the lowest range. TKE^* ($TKE^*=TKE/v_{b4}^2$) was also determined (Table 2) and highest values of TKE^* were found in the configurations with horizontal bars followed by vertical streamwise bars. Rack II and rack VI had the largest TKE^* in the bypass, while trash-racks with vertical-angled bars had significantly lower TKE^*. Considering the effects of PR and PH bar profiles, it was observed that trash-racks with PH bar profiles generated larger TKE^* values, than their associated pairs with PR bars.

3.3. Flow hydrodynamics upstream of the trash-rack

Fig. 4a and b present the cumulated frequencies distribution of the resultant velocities (v_r) and the normalized transverse velocities (v_v^*), respectively. Additionally Table 3 presents the range of the v_r parameter, their associated normalized values and the calculated normal velocities. Differences appeared for all parameters among trash-rack configurations. The shape of the distribution of different configurations was identical. Resultant velocity was the lowest at the upstream side of the trash-racks with vertical-streamwise oriented bars while rack V and rack VI had intermediate velocities (ranges v_r = 0.34-0.40 m s^{-1} and v_r = 0.41-0.46 m s^{-1}, respectively). The largest values were observed for rack IV, followed by rack III (ranges v_r at vertical-angled trash-racks= 0.58-0.67 m s^{-1}) (Fig. 4a). Considering v_v^* (Fig. 4b) at rack III and IV, the transverse velocities were mostly negative indicating a predominant countercurrent flow direction

(0.26 and 0.29, respectively on average), in contrast to the other trash-rack configurations where v_v^* were mainly oriented towards to the bypass side (average varied between -0.1 and -0.03). Related to the normal velocities all configurations provided similar values (between 0.21 and 0.23 m s^{-1}) with the highest (v_n = 0.233 m s^{-1}) for horizontal trash-racks.

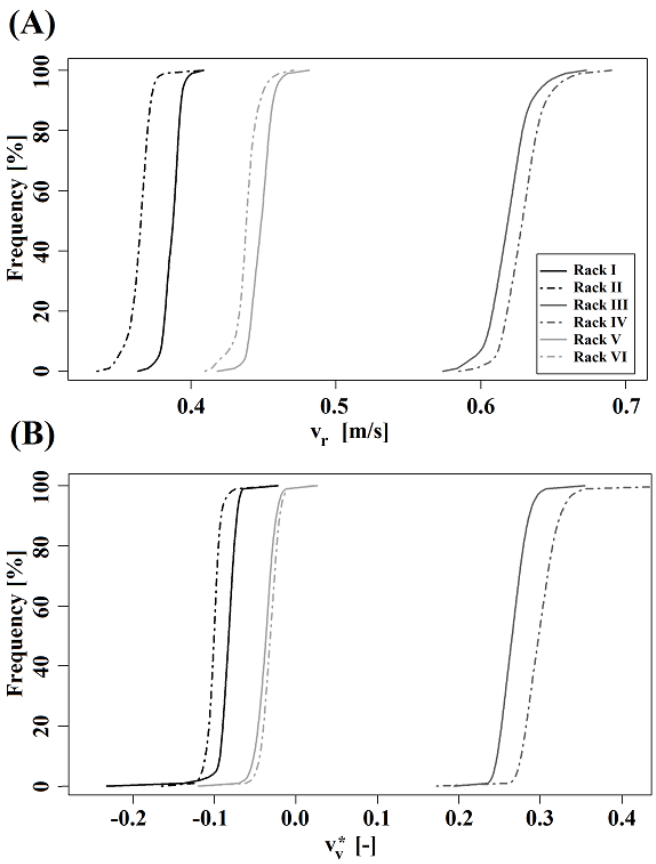

Fig 4. Cumulated frequencies of the (A) measured resultant (*v*) and the (B) normalized transverse (v_v) velocities at the upstream side of an alternative trash-rack. Data were originated from the V3V measurements from the experiments under 0.200 m^3 s^{-1} flow rate.

The normalized turbulent kinetic energy is presented in Fig. 5 and the range of *TKE* and TKE^* are presented in Table 3. The 2D planes (see Fig. 6 for the location of the planes) show the interpolated values at specific slice of the sampled volume, for horizontal and vertical planes (streamwise oriented). Variations of TKE^* in the vertical plane were minor compared to variations in the horizontal plane (Fig. 5). Differences in TKE^* were also found among experimental configurations, within the same plane. Considering the vertical plane, TKE^* was lower in experiments with rack II when comparing to rack IV and VI. For rack IV the highest values of TKE^* were observed closer to the bars, while for rack VI higher values were observed not only close to the bars but also further upstream (Fig. 5c). For the horizontal planes (0.45 z/h from the bottom), the lowest values were observed at the middle section of the slices for all the three configurations (Fig. 5d, e, f). In this plane the highest values of TKE^* were found for rack II, towards the direction of the bypass (along Y=730), while for rack IV the largest values were found at the opposite side, closest to the bar openings. The distribution of TKE^* for rack VI (Fig. 5f) differed from the remaining configurations with vertical bars. Horizontal bars were found to provide lower TKE^* areas in the horizontal plane.

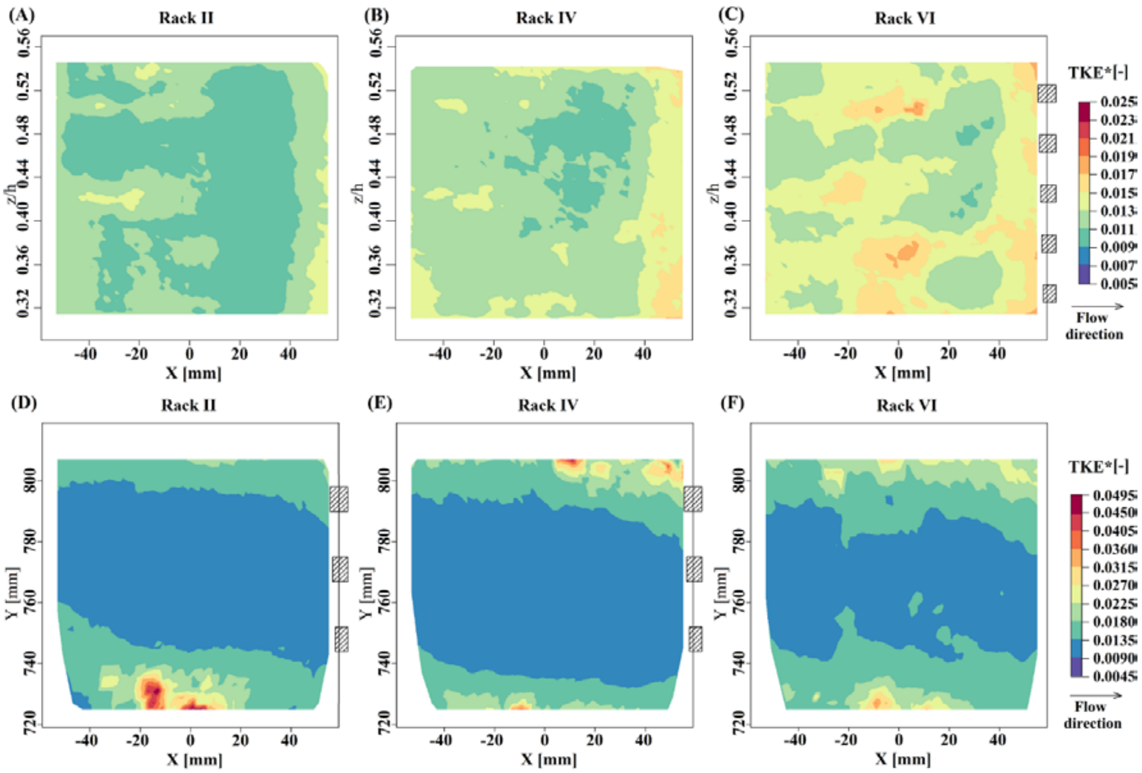

Fig 5. Interpolated TKE* fields in front of the tested trash-racks. The figures (A-C) on the top present the vertical TKE* field in 2D for (A) rack II, (B) rack IV and (C) rack VI, while the figures (D-F) on the bottom present the horizontal TKE* field in 2D for (D) rack II, (E) rack IV and (F) rack VI. The interpolation were based on the normalized turbulent kinetic energy, originated from the V3V measurements from experiments under 0.200 $m^3 s^{-1}$ flow rate. The position of the bar elements are indicated at those projections where it is relevant to show on which side the bar elements were roughly.

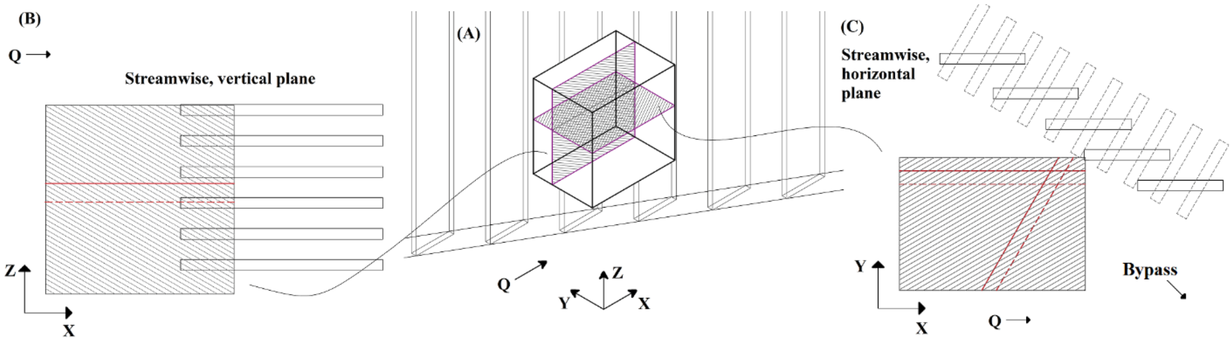

Fig. 6. V3V sampled volume and the extracted data locations. (A) The sampled V3V region at the vicinity of a trash-rack. (B) Lateral view of the streamwise, vertical 2D plane from the V3V sampled volume, beside the bar positions of the horizontal trash-rack configurations are indicated. (C) Top view of the streamwise, horizontal vertical 2D plane from the V3V sampled volume with the adjacent bar positions of the vertical-streamwise trash-rack types (continuous black lines) and bar positions of the vertical-angled trash-rack types (dashed black lines). The continuous and the dashed red lines indicate the orientation from where the acceleration values were extracted.

The range of Reynolds shear stresses within the V3V sampling volume $\tau^*_{u'v'}$ ($\tau^*_{u'v'} = \tau_{u'v'}/\rho v_{b4}^2$) and $\tau^*_{u'w'}$ are shown in Figs. 7a and 7b in terms of cumulated frequency distributions for racks II, IV and VI. The shapes of the cumulative curves are in general similar although the mean values differed. In fact, $\tau^*_{u'v'}$ for racks II and rack VI is approximately 0 ($-1.35e^{-5}$ and $7.7e^{-5}$, respectively) while the value for rack IV was one order of magnitude larger ($9.1e^{-4}$). Considering $\tau^*_{u'w'}$ the shape of the distribution for rack II differed from the shapes of the distributions for rack IV and VI indicating less variation in front of the vertical-streamwise trash-racks. The largest mean value for the streamwise vertical Reynolds shear stress was observed at rack VI (1.4e^{-3}). The lowest $\tau^*_{u'w'}$ mean value was found at rack IV (1.1e^{-3}).

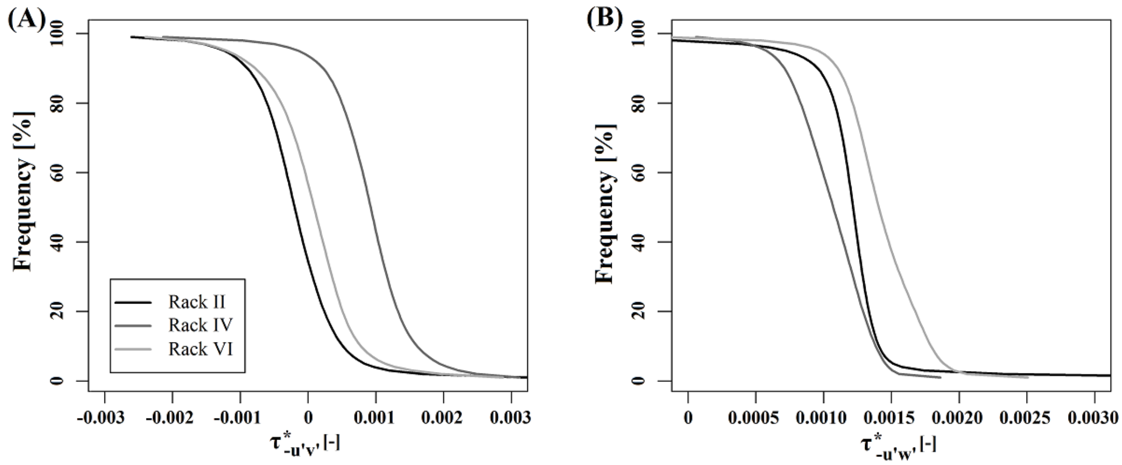

Fig. 7. Cumulated frequencies of the (A) normalized streamwise, horizontal Reynolds shear stress ($\tau^*_{u'v'}$) and the (B) normalized streamwise, vertical ($\tau^*_{u'w'}$) Reynolds shear stress at the upstream side of an alternative trash-rack. Data were originated from the V3V measurements from the experiments under 0.200 m^3 s^{-1} flow rate.

The normalized resultant accelerations ($a_r^* = a_r O_{bV}^* / v_{b4}^2$ where O_{bV}^* is the volume based blockage ratio projected on 1 m flume width, $O_{bV}^* = O_{bV} * 1\ m$) were extracted from the V3V measurements along straight lines parallel to the bar orientation (Fig. 6b and c). Such lines coincide either with the centerline of a bar element (dashed red lines on Fig. 6b, c) or pass straight through between two bars (straight red lines in Figs. 6b and 6c).

The observed acceleration patterns were similar for the tested configurations with lower accelerations further upstream of the rack and increased values at the upstream side of the bars (Fig. 8). Additionally, the maximum values of a_r and $a_r{}^*$ are presented in

Table 3. The lowest range in acceleration was found for rack II. The observed maximum acceleration was lower for both racks II and VI than for rack IV. Furthermore, different acceleration patterns were found in front and in between bars (bars-gaps, Fig. 8). Highest accelerations were found in the gaps. For both rack II and VI the acceleration through a gap evolved over 5-10 mm immediately upstream of the trash-rack, while rapid growing occurred over the last 35 mm at immediate upstream side of rack IV.

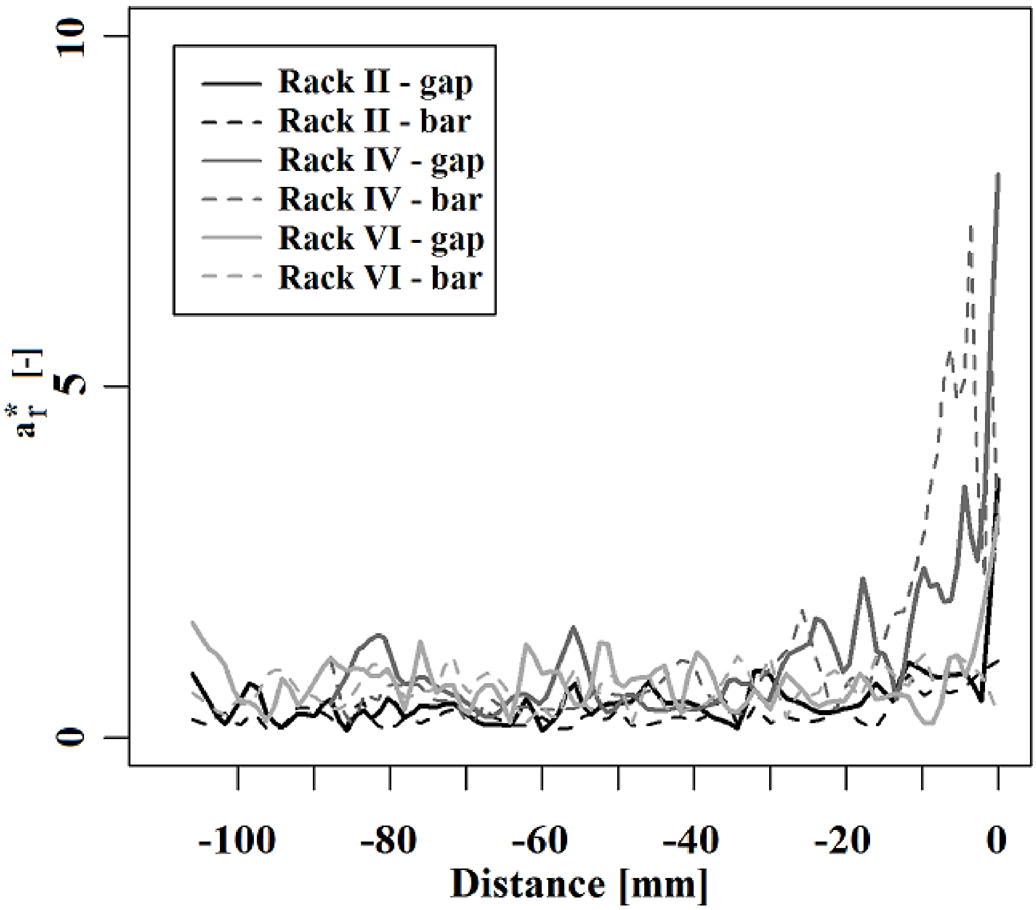

Fig. 8. Normalized acceleration (a_r^*) at the vicinity of a trash-rack towards to the bar elements. The **0** of the X axis indicates the downstream face of the V3V sampled volume. As the flow approaches the trash-rack from upstream the distance decreases. The acceleration values were extracted from the sampled volume along certain lines presented on Fig. 6B and C. The continuous lines reflect the acceleration pattern

between two bar elements, in a gap, while the dashed lines reflect the acceleration pattern towards to the centerline of a nearby bar element.

The third and fourth moments of the velocity time-series (skewness and kurtosis) were determined for configurations with aerodynamically shaped PH bar profiles (Table 4) as their associated head-loss values were always lower compared to the racks with PR bars. Considering the distributions of the measured velocities over time in a certain voxel (skewness), >90% of the data had symmetrical distribution for all three thrash-rack configurations. The remaining <10% appeared at regions closest to the bypass. In view of the kurtosis data, >75% of the data appeared as leptokurtic and there was no attributable difference among the different trash-rack types. Both presented moments were introduced in order to provide more information, therefore better understanding about the data captured by V3V. Each local minimum and maximum within the computed curl of the velocity field was detected and summarized within the sampled volume for each configuration (Table 4). Their values show some variation among the three tested configurations, with the most rotational changes occurring for rack IV, which was 31% and 46% larger than those occurring for rack II and rack VI, respectively.

4. Discussion

In this study, we analyzed the effects of three trash-rack configurations with two different bar profiles on the hydrodynamics of the flow in order to provide basic knowledge for design of fish fish-friendly trash-racks that improve downstream passage and survival of migrating fish.

Head-losses differed largely among the trach-rack designs, with highest losses for classical trash-racks (vertical-angled, rack III and IV). This is likely due to the double deflection of the flow at the angled bars (Albayrak et al., 2014). Both head-losses and head-loss coefficients were lower for racks with vertical-streamwise bars (rack I and II) and lowest for the racks with horizontal bars (rack V and VI). In accordance with Raynal et al. (2013), we found that head-losses were lower for hydrodynamic than rectangular bars. Considering both orientation, angle and bar shape the best design (horizontal hydrodynamic bars) had head-losses at 12% of the worst (vertical with angled rectangular bars). Thus, racks with the combination of horizontal and hydrodynamic bars were performing particularly well in terms of head-losses, a trait of importance for hydropower production.

The blockage ratio was calculated as the blockage in a certain volume rather than the standard method, and by doing so we also obtained estimates of the amount of material required to construct each trash-rack type and thus material costs. Blockage ratio was not correlated with the head-losses and was lowest for the vertical-streamwise racks (45-50% lower than the other trash-rack types).

The diverted portion of the total flow to the bypass also varied among trash-rack configurations and was 75-100% higher in the vertical-angled types than in the remaining tested configurations. This is likely due to the double deflection of the flow at these racks, which may have generated stronger backwater effects and additional secondary currents.

Water velocities in front of the trash-racks and at the bypass entrance varied largely among the grid designs with potential implications for fish behavior responses. The resultant velocities just in front of the racks (~105 mm to ~5) and at the bypass entrance were generally lowest for the vertical-streamwise racks while the horizontal trash-racks had the lowest velocities at the bypass entrance. In agreement with Raynal et al. (2014), that reported regions with higher velocities in front of vertical-angled trash-racks, resultant velocities were 40-70% higher in the vertical angled racks than for racks with streamwise bars (both vertical and horizontal). While both target species (Atlantic salmon and European eel) can burst swim against velocities exceeding 2 m s^{-1} (Russon and Kemp, 2011, Videler, 1993), the general recommendation to minimize risk of impingements and injury on trash-racks is that normal velocity should not exceed 0.5 m s^{-1} (DWA, 2005, Larinier, 2002). That criterion met at all of the cases. Considering resultant velocities in front of the trash-racks for the vertical-streamwise and horizontal configurations which are likely to be suitable for downstream passage of both species, whereas the vertical-angled may challenge the fish swimming capacity. While the resultant velocities exceeded 0.5 m s^{-1} at the bypass entrance for both vertical-streamwise and horizontal racks, velocity values maintained below 0.7 m s^{-1} and increased gradually trough the ramp. In contrast, higher velocities were measured in experiments with vertical-angled racks, exceeding the 0.5 m s^{-1} threshold and peaking at around at the bypass entrance. Moreover, a more rapid change of velocities was observed through the ramp at the bypass entrance, and migrating fish are known to avoid rapid changes in water velocity (Williams et al., 2012). Therefore, the hydraulic conditions created by vertical-angled racks may also challenge the success of passage through the bypass, by triggering evolved behavioral repulsion responses. Moreover, vertical-angled racks caused rather high transverse velocities immediately in front of the bars, with concurrent velocities resulting from the upcoming flow that had to turn according to the bar angle in order to flow through the trash-rack, leading to higher resistance for the approaching flow, and consequently higher Q_b. Overall, under similar structural conditions (e.g. trash-rack angle, bar spacing, bar shape) angled trash-racks with vertical-angled bars must be operated under lower flow rates to ensure lower resultant velocities.

Altering acceleration schemes both, in front of the trash-racks and at the bypass-entrance can potentially intensify negative responses by the target fish species. The convective acceleration in front of the racksand at the bypass-entrance was the lowest at rack VI while the highest was found in experiments with rack IV. Although maximums at the bars and at the bypass-entrance were found for the same rack, still, in average accelerations in the tested configurations did not exceed the threshold considered as energetically optimum for swimming performance of salmon (1 cm s^{-1} cm^{-1}, ~1 body length/s; Enders et al. (2012)) . Nevertheless, the rapid accelerations found at the vicinity of the racks for the rack III and IV, may lead to behavioral responses that can compromise downstream migration of the specimens.

The analyzed turbulence parameters are also different among trash-racks configurations. The turbulence kinetic energy (TKE) was found to be at least one order of magnitude higher at the bypass entrance than in front of the bars. This is likely to be the result of the flow contraction as the water approach to the bypass. Overall, turbulence was most abundant for the vertical-streamwise and horizontal racks. However, large variation and skewness of TKE data, in particular on the horizontal plane, may potentially bias the results. High levels of turbulent kinetic energy may hamper fish movements (Silva et al., 2011, 2012) and the present results represent a potential downside for trash-racks with horizontal bars.

Reynolds shear stresses have been regarded as one of the main turbulent parameters affecting fish swimming performance and behavior (Silva et al., 2011). Vertical-angled racks created higher values of $\tau^*_{u'v'}$ shear stress in front of the bars than any of other trash-rack configurations tested, likely a consequence of the bar orientations. Variation in $\tau^*_{u'w'}$ shear stress was lowest at the vertical-streamwise rack, both in front of the rack and at the bypass-entrance. In contrast, high variation of this parameter was found in experiments conducted with the horizontal rack with hydrodynamic bars. The wide range of negative values of negative Reynold shear stress values observed in this configurations, suggest the presence of opposite tensions acting between the streamwise and vertical direction of the flow. Such variation can be perceived by fish and may lead to repulsion of fish for those areas, because studies have been shown that fish tend to avoid areas of high Reynold shear stress (Silva et al., 2011).

It has been shown that fish swimming performance is affected by eddy characteristics such as intensity, periodicity, orientation and size (Lacey et al., 2012, Silva et al., 2012). Although we did not analyze such variables (the focus was on time-averaged data), we estimated a curling index, which reflects rotational changes averaged over time in the sampled V3V volume. This parameter could provide some insights on the degree of “chaotic flow conditions” created by the different trash-racks configurations. The particularly high curl index for the vertical-angled rack bars may be driven by the orientation of the bars, suggest that this configuration creates a more chaotic hydraulic environment than the remaining configurations. Such an environment is expecting to be more challenging for fish, by decreasing stability and creating disorientation of the fish. Moreover, such environment is likely to induce variation on the behavioral response, which may lead to deviations from the natural migratory routes.

Based on the findings of the present study and the literature Table 5 provide an overview of the trade-offs of each tested trash-racks with regards to operational and ecological criteria.

In an operational perspective, vertical-streamwise trash-rack seems to be more advantageous than the other configurations. This type of trash-racks, which requires the minimum amount of material for construction and typically fit well into existing intake channels (see EPRI, 2007; Wahl, 1992), would generate relatively low head-losses and low diverted flow to the bypasses. However, while low head-losses would be advantageous for the HPP low flow in the bypasses may be a problem for fish, both in terms of the water depth in the bypass and the proportion of water allocated to the bypass. Vertical-angled trash-racks are also regarded as easy to operate, both because ‘classical’ trash-rack cleaners or scrapers can be used and they fit better into existing channels. On the other hand, the generated head-loss and the flow diverted to the bypass would be the highest and consequently the predicted performance loss of a HPP would be maximum for this type of trash-racks. Horizontal trash-racks seems to be worse in terms of construction and maintenance. The construction of this type of trash-racks is somewhat more costly, as it requires more material. Furthermore, the maintenance of horizontal trash-racks is at present less developed, in particular in terms of available cleaning systems. Moreover, vertical-streamwise trash-racks and horizontal trash-racks diverge less flow to the bypass, which may reduce downstream passage efficiency. This may be compensated by increasing bypass area.

Indeed, from an ecological perspective horizontal trash-racks seem to be the best option to be adopted, followed by vertical-streamwise trash-racks. The hydraulic conditions (velocities, accelerations, turbulence, curl) just in front of the racks and at the bypass-entrance created by these configurations are within the thresholds that are considered to be suitable and that fit the biomechanical capacities of the target species (Atlantic salmon and Europeen eel) (Chagnaud et al., 2007, DWA, 2005, Kroese et al., 1978, Larinier, 2002, Silva et al., 2016, Williams et al., 2012). In contrast, vertical-angled trash-racks seem to perform the worst from an ecological perspective. The high velocities and strong accelerations originated by these type of racks may trigger evolved behavioral responses in fish, which may disrupt their migratory pattern, causing delays, increased risk of predation and increasing swimming cost. Furthermore, these high velocities would increase risk of impingement, injury or mortality of fish on the trash-racks. Contrarily, the effects on fish of high velocities and accelerations at the top of the ramp can be deemed as twofold at the bypass-entrance, as these hydraulic conditions may also help fish to move downstream. If acceleration would exceed maximum fish swimming capacity, then fish may be drift downstream to the bypass. Such type of behavior was observed in Silva et al. (2016), in their study on the effects different designs of spillways on the downstream behavior of the Iberian barbel and the European eels. They found that above a certain velocity threshold, fish swimming capacity and stability were compromised leading to the reduction in control and the consequent drifting over the spillway of individual of both species with different biomechanical skills. The high turbulent conditions both at the trash-racks and at the bypass entrance created by vertical-angled trash-racks may also be a problem for downstream migration of fish. High levels of turbulence and the chaotic flow dynamics (herein expressed as curl) may induce loss of stability and disorientation, deviations of the rheotaxis orientation and the migratory routes of fish (Enders et al., 2012, Lacey et al., 2012, Silva et al., 2012, Wilkes et al., 2017). To improve their ecological performance vertical-angled trash-racks need to be operated under lower flow discharges, what can have grave repercussions for the HPP.

In summary, our findings combined with the existent literature suggest the horizontal trash-racks followed by vertical-streamwise trash-racks as the best candidates for fish-friendly trash-racks that also imply minimum additional costs for the HPP. It is likely that the maintenance challenges can be solved by for example developing designated cleaning systems for horizontal bar racks.

AKNOWLEDGEMENTS

This research was supported by the SafePass project (no. 244022) funded by the Research Council of Norway (RCN) under the ENERGIX program. We thank the technical staff of the Department of Civil and Environmental Engineering, at the NTNU.

REFERENCES

ADAM, B. & BRUIJS, M. C. M. 2006. General requirements of fish protection and downstream migration facilities investigations on the river Meuse system In Free Passage for Aquatic Fauna in Rivers and Other Water Bodies. International DWA Symposium on Water Resources Management, Berlin, Germany.

ALBAYRAK, I., KRIEWITZ, C. R., HAGER, W. H. & BOES, R. M. 2017. An experimental investigation on louvres and angled bar racks. *Journal of Hydraulic Research***,** 1-17.

ALBAYRAK, I., KRIEWITZ, C. R., HAGER, W. H. & BOES, R. M. 2017. An experimental investigation on louvres and angled bar racks. *Journal of Hydraulic Research***,** 1-17.

AMARAL, S. V., WINCHELL, F. C., MCMAHON, B. J. & DIXON, D. A. 2002. Evaluation of angled bar racks and louvers for guiding silver phase American eels. *Biology, Management, and Protection of Catadromous Eels,* 33**,** 367-376.

BARBIER, C. & HUMPHREY, J. A. C. 2009. Drag force acting on a neuromast in the fish lateral line trunk canal. I. Numerical modelling of external-internal flow coupling. *Journal of the Royal Society Interface,* 6**,** 627-640.

BOES, R., ALBAYRAK, I., KRIEWITZ, C. R. & PETER, A. 2016. Fish Protection and Downstream Fish Migration by Means of Guidance Systems with Vertical Bars: Head Loss and Bypass Efficiency. *Wasserwirtschaft,* 106**,** 29-35.

BOUBEE, J. A. T. & WILLIAMS, E. K. 2006. Downstream passage of silver eels at a small hydroelectric facility. *Fisheries Management and Ecology,* 13**,** 165-176.

BRUIJS, M. C. M. & DURIF, C. M. F. 2009. Silver Eel Migration and Behaviour. *In:* VAN DEN THILLART, G., DUFOUR, S. & RANKIN, J. C. (eds.) *Spawning*

Migration of the European Eel: Reproduction Index, a Useful Tool for Conservation Management. Dordrecht: Springer Netherlands.

CALLES, O. & GREENBERG, L. 2009. Connectivity Is a Two-Way Street-the Need for a Holistic Approach to Fish Passage Problems in Regulated Rivers. *River Research and Applications,* 25**,** 1268-1286.

CALLES, O., KARLSSON, S., HEBRAND, M. & COMOGLIO, C. 2012. Evaluating technical improvements for downstream migrating diadromous fish at a hydroelectric plant. *Ecological Engineering,* 48**,** 30-37.

CALLES, O., KARLSSON, S., VEZZA, P., COMOGLIO, C. & TIELMAN, J. 2013. Success of a low-sloping rack for improving downstream passage of silver eels at a hydroelectric plant. *Freshwater Biology,* 58**,** 2168-2179.

CHAGNAUD, B. P., BLECKMANN, H. & HOFMANN, M. H. 2007. Karman vortex street detection by the lateral line. *Journal of Comparative Physiology a-Neuroethology Sensory Neural and Behavioral Physiology,* 193**,** 753-763.

DRUCKER, E. G. & LAUDER, G. V. 1999. Locomotor forces on a swimming fish: Three-dimensional vortex wake dynamics quantified using digital particle image velocimetry. *Journal of Experimental Biology,* 202**,** 2393-2412.

DWA, 2005. Fish Protection Technologies and Downstream Fishways. Dimensioning, Design, Effectiveness Inspection. Hennef, DWA German Association for Water, Wastewater and Waste

ENDERS, E. C., BOISCLAIR, D. & ROY, A. G. 2003. The effect of turbulence on the cost of swimming for juvenile Atlantic salmon (Salmo salar). *Canadian Journal of Fisheries and Aquatic Sciences,* 60**,** 1149-1160.

ENDERS, E. C., GESSEL, M. H., ANDERSON, J. J. & WILLIAMS, J. G. 2012. Effects of Decelerating and Accelerating Flows on Juvenile Salmonid Behavior. *Transactions of the American Fisheries Society,* 141**,** 357-364.

EPRI, 2007. Hydropower Technology Roundup Report: Trash and Debris Management at Hydroelectric Facilities, TR-113584-V10. HCI.

GORING, D. G. & NIKORA, V. I. 2002. Despiking acoustic Doppler velocimeter data. *Journal of Hydraulic Engineering-Asce,* 128**,** 117-126.

HINDAR, K., GALLAUGHER, P. & WOOD, L. 2003. Wild Atlantic salmon in Europe: status and perspectives. In: Proceedings from the World Summit on Salmon (Gallagher, P. & Wood, I., eds), pp. 47–52. Vancouver, BC: Simon Fraser University.

ICES, 2001. Report of the EIFAC ⁄ ICES Working Group on Eels. ICES, CM 2001 ⁄ ACFM:03, Copenhagen , 87 p.

KROESE, A. B. A., VANDERZALM, J. M. & VANDENBERCKEN, J. 1978. Frequency-Response of Lateral-Line Organ of Xenopus-Laevis. *Pflugers Archiv-European Journal of Physiology,* 375**,** 167-175.

KROESE, A. B. A. & SCHELLART, N. A. M. 1992. Velocity-Sensitive and Acceleration-Sensitive Units in the Trunk Lateral Line of the Trout. *Journal of Neurophysiology,* 68**,** 2212-2221.

LACEY, R. W. J., NEARY, V. S., LIAO, J. C., ENDERS, E. C. & TRITICO, H. M. 2012. The Ipos Framework: Linking Fish Swimming Performance in Altered Flows from Laboratory Experiments to Rivers. *River Research and Applications,* 28**,** 429-443.

LANE S.N., BIRON P.M., BRADBROOK K.F., BUTLER J.B., CHANDLER J.H., CROWELL M.D., MCLELLAND S.J., RICHARDSK.S. & ROY A.G. 1998. Three-dimensional measurement of river channel flow processes using acousticDoppler velocimetry. Earth Surface Processes and Landforms 23, 1247–1267.

LARINIER M. 2001. Environmental issues, dams and fish migration. In: G. Marmulla (ed.) Dams, Fish and Fisheries. Opportunities, Challenges and Conflict Resolution. Rome: FAO Fisheries Technical Paper No. 419, pp. 45–90

LARINIER, M. 2008. Fish passage experience at small-scale hydro-electric power plants in France. *Hydrobiologia,* 609**,** 97-108.

LARINIER, M., TRAVADE, F., PORCHER., 2002: Fishways: biological basis, design criteria and monitoring. Bull. Fr. Peche Piscic., 364 suppl., 208p. ISBN 92-5-104665-4.

LIAO, J. C. 2007. A review of fish swimming mechanics and behaviour in altered flows. *Philosophical Transactions of the Royal Society B-Biological Sciences,* 362**,** 1973-1993.

LUNDQVIST, H., RIVINOJA, P., LEONARDSSON, K. & MCKINNELL, S. 2008. Upstream passage problems for wild Atlantic salmon (Salmo salar L.) in a regulated river and its effect on the population. *Hydrobiologia,* 602**,** 111-127.

MARTIGNAC, F., BAGLINIERE, J. L., THIEULLE, L., OMBREDANE, D. & GUILLARD, J. 2013. Influences of a dam on Atlantic salmon (Salmo salar) upstream migration in the Couesnon River (Mont Saint Michel Bay) using hydroacoustics. *Estuarine Coastal and Shelf Science,* 134**,** 181-187.

MATLAB and Statistics Toolbox Release 2016a, The MathWorks, Inc., Natick, Massachusetts, United States.

MCLELLAND S.J. & NICHOLAS A.P. 2000. A new method for evaluating errors in high-frequency ADVmeasurements. Hydrological Processes 14, 351–366.

MOSONYI, E. 1991. Water power development. 2 A, High-head power plants, 3rd enl. and completely rev. ed. Budapest : Akadémiai Kiadó, 1991

NEZU, I., NAKAWAGA, H. 1993. Turbulence in open-channel flows. A.A. Balkema, Rotterdam, Netherlands

NYQVIST, D., NILSSON, P. A., ALENÄS, I., ELGHAGEN, J., HEBRAND, M., KARLSSON, S., KLÄPPE, S. & CALLES, O. 2017. Upstream and downstream passage of migrating adult Atlantic salmon: Remedial measures improve passage performance at a hydropower dam. *Ecological Engineering,* 102**,** 331-343.

POTHOS, S., TROOLIN, D., LAI, W. & MENON, R. 2009. V3v –Volumetric Three-Component Velocimetry For 3dFlow Measurements-Main Principle, Theory And Applications. Termotehnica, 2, 25-32.

R DEVELOPMENT CORE TEAM 2017. R: A language and environment for statistical computing. Vienna, Austria: R Foundation for Statistical Computing.

RAYNAL, S., CHATELLIER, L., COURRET, D., LARINIER, M. & DAVID, L. 2013. An experimental study on fish-friendly trashracks - Part 2. Angled trashracks. *Journal of Hydraulic Research,* 51**,** 67-75.

RAYNAL, S., CHATELLIER, L., COURRET, D., LARINIER, M. & DAVID, L. 2014. Streamwise bars in fish-friendly angled trashracks. *Journal of Hydraulic Research,* 52**,** 426-431.

RUSSON, I. J. & KEMP, P. S. 2011. Experimental quantification of the swimming performance and behaviour of spawning run river lamprey Lampetra fluviatilis and European eel Anguilla anguilla. *Journal of Fish Biology,* 78**,** 1965-1975.

SILVA, A. T., SANTOS, J. M., FERREIRA, M. T., PINHEIRO, A. N. & KATOPODIS, C. 2011. Effects of Water Velocity and Turbulence on the Behaviour of Iberian Barbel (Luciobarbus Bocagei, Steindachner 1864) in an Experimental Pool-Type Fishway. *River Research and Applications,* 27**,** 360-373.

SILVA, A. T., KATOPODIS, C., SANTOS, J. M., FERREIRA, M. T. & PINHEIRO, A. N. 2012. Cyprinid swimming behaviour in response to turbulent flow. *Ecological Engineering,* 44**,** 314-328.

SILVA, A. T., KATOPODIS, C., TACHIE, M. F., SANTOS, J. M. & FERREIRA, M. T. 2016. Downstream Swimming Behaviour of Catadromous and Potamodromous Fish Over Spillways. *River Research and Applications,* 32**,** 935-945.

TRITICO, H. M. 2009. *The effects of turbulence on habitat selection and swimming kinematics of fishes.* Dissertation/Thesis, ProQuest Dissertations Publishing.

TSIKATA, J. M., TACHIE, M. F. & KATOPODIS, C. 2009. Particle Image Velocimetry Study of Flow near Trashrack Models. *Journal of Hydraulic Engineering-Asce,* 135**,** 671-684.

TSIKATA, J. M., TACHIE, M. F. & KATOPODIS, C. 2014. Open-channel turbulent flow through bar racks. *Journal of Hydraulic Research,* 52**,** 630-643.

VIDELER, J.J. 1993. Fish swimming: London, United Kingdom, Chapman and Hall.

WAHL, T. 2002. Analyzing ADV Data Using WinADV. In: Joint Conference on Water Resource Engineering and Water Resources Planning and Management 2000, July 30-August 2, 2000, Minneapolis, Minnesota, United States

WAHL, T.L. 1992. Trash Control Structures and Equipment: A Literature Review and Survey of Bureau of Reclamation Experience. Denver, Colorado.

WILKES, M. A., ENDERS, E. C., SILVA, A. T., ACREMAN, M. & MADDOCK, I. 2017. Position choice and swimming costs of juvenile Atlantic salmon salmo salar in turbulent flow. *Journal of Ecohydraulics***,** 1-12.

WILLIAMS, J. G., ARMSTRONG, G., KATOPODIS, C., LARINIERE, M. & TRAVADE, F. 2012. Thinking Like a Fish: A Key Ingredient for Development of Effective Fish Passage Facilities at River Obstructions. *River Research and Applications*, 28**,** 407-417.

Table 1

Detailed information about the experimental setup: bar orientation, profile of the tested trash-racks, volume based blockage ratio (O_{bV}), bulk velocities (v_{b4}) at the furthest cross-section (P_4), with the associated bar Reynolds number (Re_b) and percentage of flow discharge in the bypass (Q_b). The values were obtained from experiments under 0.200 $m^3 s^{-1}$ flow discharge.

	Bar-setup	Profile	O_{bV} [-]	v_{b4} [m s^{-1}]	Re_b [-]	Q_b [%]
Rack I	Vertical-streamwise	PR	0.18	0.395	3163	4.1
Rack II	Vertical-streamwise	PH	0.16	0.394	3151	3.2
Rack III	Vertical-angled	PR	0.34	0.388	3103	7.3
Rack IV	Vertical-angled	PH	0.30	0.388	3100	6.4
Rack V	Horizontal	PR	0.35	0.395	3160	4.0
Rack VI	Horizontal	PH	0.32	0.398	3184	3.1

Table 2

Mean acceleration (a_r), vertical Reynolds shear stress $\tau^*_{u'w'}$ and TKE^* at the entrance of the bypass section, based on the ADV measurements. The values were obtained from experiments under 0.200 $m^3 s^{-1}$ flow discharge.

	a_r [m s^{-2}]			$\tau^*_{u'w'}$			TKE^*		
	Mean	Min	Max	Mean#	Min#	Max#	Mean#	Min#	Max#
Rack I	0.199	0.038	1.174	0.27	-3.18	2.83	56.3	38.9	100.4
Rack II	0.143	0.021	0.817	0.15	-2.68	1.97	111.5	70.7	151.0
Rack III	0.411	0.090	1.319	0.60	-3.14	4.42	52.7	20.2	94.7
Rack IV	0.530	0.062	1.249	-0.09	-3.35	4.31	60.1	18.0	130.3
Rack V	0.165	0.014	0.818	-0.74	-9.28	2.40	91.8	56.8	126.5
Rack VI	0.128	0.016	0.618	-0.41	-7.30	3.41	182.2	110.2	251.2

#multiplied by 10^3

Table 3

Measured and normalized values of mean velocities [m s^{-1}], normal velocities [m s^{-1}] along the range of the turbulent kinetic energy [$m^2 s^{-2}$] and the maximum accelerations [m s^{-2}] originated by the V3V measurements. The values were obtained from experiments under 0.200 $m^3 s^{-1}$ flow discharge.

	v_r [m s^{-1}]	v_r^*	v_n [m s^{-1}]	TKE [$m^2 s^{-2}$]	TKE^*	a_r [m s^{-2}]	a_r^*
	Mean	Mean	Mean	Range#	Range#	Max	Max
Rack I	0.38	0.96	0.217	-	-	-	-
Rack II	0.36	0.91	0.216	1.4-2.3 1.4-7.0##	9.0-15.0 9.0-45.0##	3.64 1.08###	3.70 1.10###
Rack III	0.62	1.60	0.216	-	-	-	-
Rack IV	0.63	1.62	0.212	1.4-2.6 1.4-6.8##	9.0-17.0 9.0-45.0##	4.01 1.46###	8.00 2.91###
Rack V	0.45	1.13	0.233	-	-	-	-
Rack VI	0.44	1.11	0.231	1.4-3.3 1.4-5.1##	9.0-21.0 9.0-32.0##	1.56 0.16###	3.15 0.32###

#multiplied by 10^3

##values from the horizontal plane

###values from the bar oriented accelerations

Table 4
The Mean values of skewness and kurtosis and index of the curl (*N*) for racks II, IV and VI, under flow discharge of 0.200 $m^3 s^{-1}$.

	Skewness [-]			Kurtosis [-]			Curl [*N*]
	Mean	Min	Max	Mean	Min	Max	I_{mi-ma}
Rack II	-0.339	-9.608	0.390	9.24	2.71	171.16	898
Rack IV	0.000	-4.219	0.455	4.92	2.34	54.38	1179
Rack VI	-0.327	-8.822	0.331	8.27	2.71	157.59	808

Table 5
Summary of the operational (o) and ecological (e) advantages and disadvantages of each tested trash-racks for the development of fish-friendly structures.

Subjects		Vertical-streamwise trash-racks (Rack I-II)	Vertical-angled trash-racks (Rack III-IV)	Horizontal trash-racks (Rack V-VI)
Operational questions	Required material	+		–
	Maintenance complexity	–	+	–
	Retrofitted built in	+	+	–
	Head-losses	+	–	+
	Diverted discharge	+ (o) /–(e)	– (o) / + (e)	+ (o) / – (e)
Bypass section[#]	Velocities	+	+	+
	Accelerations	+	+/–	+
	Turbulence	+	–	+
Upstream of the racks[#]	Velocities	+	–	+
	Accelerations	+	–	+
	Turbulence + Curl		–	+

[#]Based on the literature existent for salmon and eel // + recommended/advantageous – not recommended/disadvantageous +/- under certain conditions